1. Overview

The CP-even fraction $F_+^{4\pi}$ of 4π can be determined through the evaluation of

$$M_i^{K^0_S\pi\pi} = h_{K^0_S\pi\pi}(T_i^{K^0_S\pi\pi} + T_{-i}^{K^0_S\pi\pi} - 2\,c_i\sqrt{T_i^{K^0_S\pi\pi}T_{-i}^{K^0_S\pi\pi}}\,(2F_+^{4\pi} - 1)) \tag{1.1}$$

and

$$M_i^{K^0_L\pi\pi} = h_{K^0_L\pi\pi}(T_i^{K^0_L\pi\pi} + T_{-i}^{K^0_L\pi\pi} + 2\,c_i\sqrt{T_i^{K^0_L\pi\pi}T_{-i}^{K^0_L\pi\pi}}\,(2F_+^{4\pi} - 1)) \tag{1.2}$$

where the M_i denote the number of events in bin i of the $K^0_S\pi\pi$/ $K^0_L\pi\pi$ Dalitz-Plot tagged against 4π, the T_i the relative amount of events in bin i of flavour-tagged $K^0_S\pi\pi$/ $K^0_L\pi\pi$ Dalitz-Plot and the h are normalisation factors.
By summing over the bins i and $-i$ these expressions become

$$MM_i^{K^0_S\pi\pi} = M_i^{K^0_S\pi\pi} + M_i^{K^0_S\pi\pi} = 2\cdot h_{K^0_S\pi\pi}(T_i^{K^0_S\pi\pi} + T_{-i}^{K^0_S\pi\pi} - 2\,c_i\sqrt{T_i^{K^0_S\pi\pi}T_{-i}^{K^0_S\pi\pi}}\,(2F_+^{4\pi} - 1)) \tag{1.3}$$

and

$$MM_i^{K^0_L\pi\pi} = M_i^{K^0_L\pi\pi} + M_{-i}^{K^0_L\pi\pi} = 2\cdot h_{K^0_L\pi\pi}(T_i^{K^0_L\pi\pi} + T_{-i}^{K^0_L\pi\pi} + 2\,c_i\sqrt{T_i^{K^0_L\pi\pi}T_{-i}^{K^0_L\pi\pi}}\,(2F_+^{4\pi} - 1)) \tag{1.4}$$

The following report summarised how the values for $MM_i^{K^0_S\pi\pi}$ and $MM_i^{K^0_L\pi\pi}$ are determined.

2. Binned $K^0_S\pi\pi$ vs 4π yields

2.1 Overview

The values for MM_i are obtained using:

$$MM_i = (N_i^{meas} - B_i^{peak} - B_i^{flat})/\epsilon_i \tag{2.1}$$

MM_i : absolute number of 4π vs $K^0_S\pi\pi$ events in bin i. This is the quantity that enters the fit for F_+.
N_i^{meas} : total number of reconstructed and selected events in bin i.
B_i^{peak} : number of reconstructed and selected peaking bkg. events in bin i. The only peaking bkg. expected is $K^0_S\pi\pi$ vs $K^0_S\pi\pi$.
B_i^{flat} : number of reconstructed and selected flat bkg. events in bin i.
ϵ_i : reconstruction and selection efficiency for 4π vs $K^0_S\pi\pi$ events in bin i.

2.2 Absolut number of 4π vs $K^0_S\pi\pi$ events

The selection of 4π vs $K^0_S\pi\pi$ was done as outlined in Chris' report. The resulting numbers are listed below.

bin i	$N_i^{meas} \pm \sqrt{N_i^{meas}}$
1	38 ± 6.16
2	22 ± 4.69
3	21 ± 4.58
4	12 ± 3.46
5	59 ± 7.68
6	24 ± 4.90
7	30 ± 5.48
8	42 ± 6.48

Table 2.1: *Number N_i^{meas} of reconstructed 4π vs $K^0_S\pi\pi$ events summed over bin i and -i. The errors are taken as $\sqrt{N_i^{meas}}$.*

2.3 Determination of number of peaking background events

It is assumed that the only peaking bkg to $K^0_S\pi\pi$ vs 4π is $K^0_S\pi\pi$ vs $K^0_S\pi\pi$.
The number of peaking bkg events in bin i B_i^{peak} is determined from

$$B_i^{peak} = B_{tot}^{peak} \cdot a_i^{peak} \tag{2.2}$$

where B_{tot}^{peak} denotes the total number of $K^0_S\pi\pi$ vs $K^0_S\pi\pi$ events in the selected data sample and a_i^{peak} the percentage of $K^0_S\pi\pi$ vs $K^0_S\pi\pi$ events in bin i.

2.3.1 Total number of peaking background events in selected data sample

The total number of peaking bkg events in the selected sample is determined using the generic MC. The same reconstruction and selection as to the data is applied to the generic MC. This results in 60 ± 7.75 and 243 ± 15.59 selected $K^0_S\pi\pi$ vs $K^0_S\pi\pi$ events in the lumix10 and lumix20 sample respectively (the errors are taken to be the sqrt of the yields). These numbers are then scaled appropriately to give the expected number of total bkg events in the reconstructed data sample and no error on the scaling factors is assumed.

$$B_{tot}^{peak} = 0.105 \cdot 60 + 0.05 \cdot 243 = 18.45 \pm 1.13 \tag{2.3}$$

2.3.2 Relative amount of peaking background events per bin

Since the generic MC has been generated without taking into account the quantum correlations and no model-dependence should be introduced to the analysis, the relative amount of peaking bkg events per bin has to be determined with data.
Therefore the CLEO data is reconstructed and selected in the same way as for the signal decay, apart from a 'reversed K^0_S veto'. This means that instead of rejecting events where two of the pions from the 4π have a K^0_S flight significance >0, events with a K^0_S flight significance >2 are selected to ensure a reasonably clean $K^0_S\pi\pi$ vs $K^0_S\pi\pi$ sample. The percentage of these events per bin is listed below.

bin i	a_i^{peak} [%]
1	23.84 ± 3.47
2	9.93 ± 2.43
3	10.60 ± 2.50
4	3.31 ± 1.46
5	15.89 ± 2.98
6	8.61 ± 2.28
7	9.93 ± 2.43
8	17.88 ± 3.12

Table 2.2: *Relative amount of $K^0_S\pi\pi$ vs $K^0_S\pi\pi$ events per bin.*

2.3.2.1 Cleanness of $K^0_S\pi\pi$ vs $K^0_S\pi\pi$ sample

The gen MC suggest that the 'reversed K^0_S veto' yields a sample of 96% $K^0_S\pi\pi$ vs $K^0_S\pi\pi$ events. A systematic should be assigned to account effect of the other 4%.

2.3.2.2 Selection-bias

Unfortunately 'reversed K^0_S veto' introduced a bias in the distribution of expected $K^0_S\pi\pi$ vs $K^0_S\pi\pi$ events over the bins. Figure 2.1 shows the distribution of $K^0_S\pi\pi$ vs $K^0_S\pi\pi$ events over the bins for the selection with the K^0_S-Veto and the 'reversed K^0_S veto' on $K^0_S\pi\pi$ vs $K^0_S\pi\pi$ signal MC.

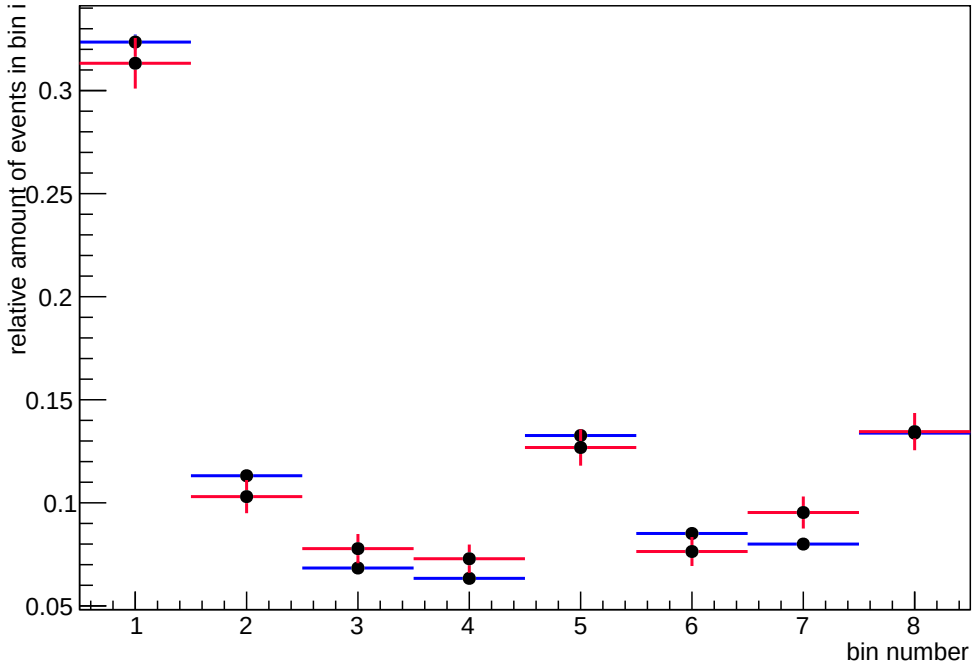

Figure 2.1: *Distribution of $K^0_S\pi\pi$ vs $K^0_S\pi\pi$ events over the bins determined by using $K^0_S\pi\pi$ vs $K^0_S\pi\pi$ MC. Blue: reversed K^0_S veto cut of FS>2, red: K^0_S veto cut of FS<0 as is used in the data sample.*

To compensate for this bias the values in Table 2.2 are being weighted with the ratio of reversed K^0_S veto over the K^0_S veto efficiencies determined from the $K^0_S\pi\pi$ vs $K^0_S\pi\pi$ signal MC sample. The weighting factors are listed below.

bin i	*weight*
1	0.97 ± 0.04
2	0.91 ± 0.07
3	1.14 ± 0.11
4	1.15 ± 0.11
5	0.96 ± 0.07
6	0.90 ± 0.09
7	1.19 ± 0.10
8	1.01 ± 0.07

Table 2.3: *Amount by which the numbers in Table 2.2 have to be weighted to compensate for the bias induced by the Ks-Selection cut.*

2.3.3 Resulting number of peaking background events in selected data sample

Applying these scaling values to the factors a_i yields the total amount of $K^0_S\pi\pi$ vs $K^0_S\pi\pi$ contamination in the data sample listed below.

bin i	B_i^{peak}	B_i^{peak} w/o removal of selection bias
1	4.26 ± 0.69	4.40 ± 0.69
2	1.67 ± 0.44	1.83 ± 0.46
3	2.22 ± 0.58	1.95 ± 0.48
4	0.70 ± 0.32	0.61 ± 0.27
5	2.80 ± 0.59	2.93 ± 0.58
6	1.43 ± 0.41	1.59 ± 0.43
7	2.18 ± 0.58	1.83 ± 0.46
8	3.32 ± 0.66	3.30 ± 0.61

Table 2.4: *Number of peaking background events per bin in the data sample before bias correction.*

2.4 Determination of number of flat background events

The number of flat bkg events is determined using the usual sidebands (denoted A, B, C and D). The number of events in the sidebands is extrapolated to give the amount of flat bkg in the signal region using the equation

$$B_{tot}^{flat} = \frac{a_S}{a_D} N_D + \sum_{j=A,B,C} \frac{a_S}{a_j}(N_j - \frac{a_j}{a_D} N_D) \tag{2.4}$$

where N_j is the number of events in sideband j, a_j is the area of sideband j and a_S is the area of the signal region. The results are listed below (no errors are assumed on the values of a_j).

N_A	1 ± 1
N_B	0 ± 1
N_C	20 ± 4.47
N_D	2 ± 1.41
B_{tot}^{flat}	11.64 ± 2.90

Table 2.5: *Number of flat bkg in the sideband and extrapolated to the signal region.*

To get the number of flat bkg events in bin i, the relative area of bin i is determined using the `dkpp_babar.root` histogram. Assuming no error on the relative area of bin i the number of flat bkg events are:

bins	number of flat bkg events
1	3.85 ± 1.13
2	1.33 ± 0.39
3	0.74 ± 0.22
4	0.69 ± 0.20
5	1.55 ± 0.45
6	0.94 ± 0.28
7	0.98 ± 0.29
8	1.56 ± 0.46

Table 2.6: *Number of flat bkg events per bin.*

2.5 Determination of the signal selection-efficiency

The signal selection efficiency in each bin is determing using a sample of 266998 $K^0_S\pi\pi$ vs 4π signal MC events.
The results are listed below.

bin	ϵ [%]
1	16.12 ± 0.12
2	15.94 ± 0.21
3	18.29 ± 0.30
4	17.24 ± 0.30
5	16.40 ± 0.20
6	17.02 ± 0.26
7	16.20 ± 0.25
8	16.69 ± 0.20

Table 2.7: *Signal efficiency per bin.*

2.6 Resulting MM_i

Since M_i and M_{-i} are the same, the numbers are directly evaluated for the sum of M_i and M_{-i} and listed on the table below.

bin	MM_i
1	185.4 ± 39.1279
2	119.238 ± 29.702
3	98.6176 ± 25.3428
4	61.5508 ± 20.244
5	333.144 ± 47.2163
6	127.08 ± 28.9874
7	165.695 ± 34.1484
8	222.469 ± 39.2218

Table 2.8: M_i + M_{-i}

3. Binned $K^0_{\rm L}\pi\pi$ vs 4π yields

3.1 Overview

The values for MM_i are obtained using:

$$MM_i = (N_i^{meas} - B_i^{peak} - B_i^{flat} - B_i^{cont})/\epsilon_i \tag{3.1}$$

MM_i : absolute number of 4π vs $K^0_{\rm L}\pi\pi$ events in bin i. This is the quantity that enters the fit for F_+.
N_i^{meas} : total number of reconstructed and selected events in bin i.
B_i^{peak} : number of reconstructed and selected peaking bkg. events in bin i.
B_i^{flat} : number of reconstructed and selected flat bkg. events in bin i.
B_i^{cont} : number of reconstructed and selected continuum bkg. events in bin i.
ϵ_i : reconstruction and selection efficiency for 4π vs $K^0_{\rm L}\pi\pi$ events in bin i.

3.2 Absolute number of 4π vs $K^0_{\rm L}\pi\pi$ events

The selection of 4π vs $K^0_{\rm L}\pi\pi$ was done as outlined in Chris' report. The resulting numbers are listed below.

bin i	$N_i^{meas} \pm \sqrt{N_i^{meas}}$
1	154 ± 12.41
2	59 ± 7.68
3	50 ± 7.07
4	23 ± 4.80
5	50 ± 7.07
6	28 ± 5.29
7	71 ± 8.43
8	77 ± 8.77

Table 3.1: *Number N_i^{meas} of reconstructed 4π vs $K^0_{\rm L}\pi\pi$ events summed over bin i and -i. The errors are taken as $\sqrt{N_i^{meas}}$.*

3.3 Determination of number of peaking background events

Three decays are identified as peaking bkg (peaking in missing mass squared) for $K^0_L\pi\pi$ vs 4π using the gen MC (see Figure 3.1):

- $K^0_L\pi\pi$ vs $K^0_S\pi\pi$: 8% of the events in the signal window
- $K^0_S\pi\pi$ vs 4π: 1.9% of the events in the signal window
- $K^0_S\pi\pi$ vs $K^0_S\pi\pi$: 0.3% of the events in the signal window

(signal window: $0.2\,GeV^2 <$ miss. mass sq $< 0.3\,GeV^2$). Due to the very low contribution the $K^0_S\pi\pi$ vs $K^0_S\pi\pi$ bkg is being neglected (at first, we can change that if we want to).

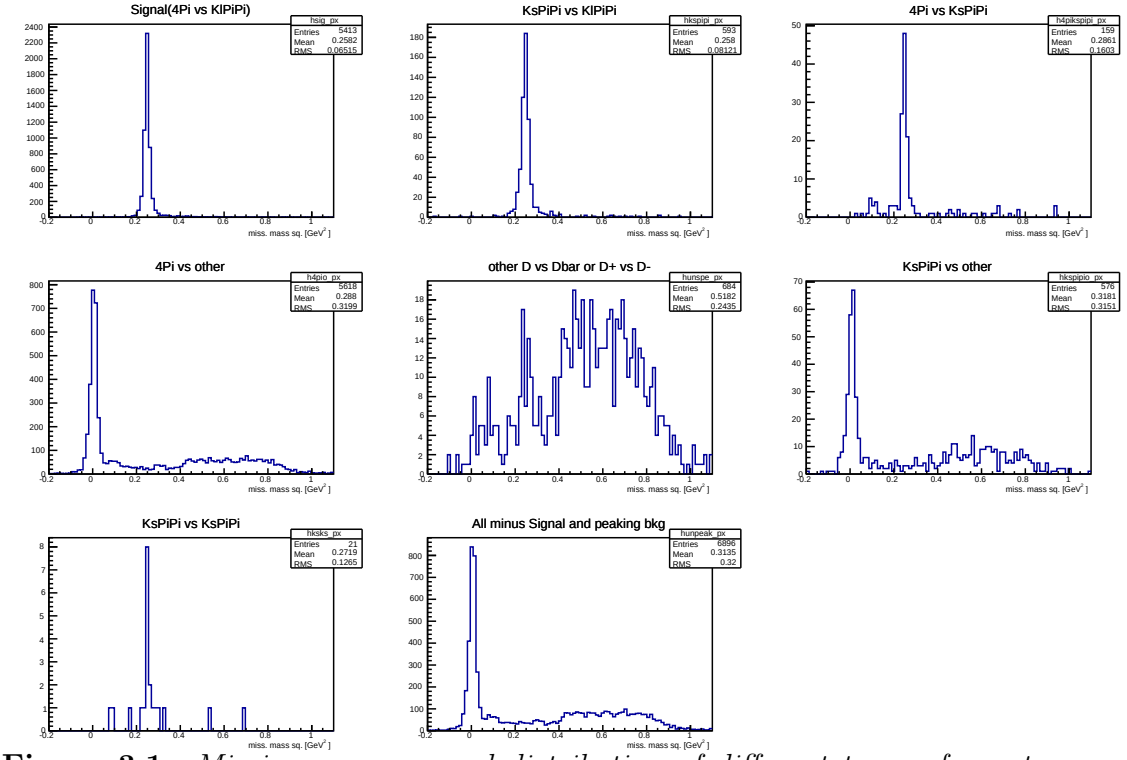

Figure 3.1: *Missing mass squared distribution of different types of events reconstructed as $K^0_L\pi\pi$ vs 4π according to the gen MC.*

As for the $K^0_S\pi\pi$ vs 4π the number of peaking bkg events per bin is determined from

$$B_i^{peak} = B_{tot}^{peak} \cdot a_i^{peak} \tag{3.2}$$

for both bkgs separately, where B_{tot}^{peak} denotes the total number of peaking bkg events in the selected data sample and a_i^{peak} the percentage of peaking bkg events in bin i.

3.3.1 Total number of peaking background events in selected data sample

The total number of peaking bkg events in the selected sample is determined using the generic MC. The same reconstruction and selection as to the data is applied to the generic MC. This results in 98 ± 9.90 and 419 ± 20.47 selected $K^0_L\pi\pi$ vs $K^0_S\pi\pi$ events in the lumix10 and lumix20 sample respectively and 15 ± 3.87 and 90 ± 9.49 $K^0_S\pi\pi$ vs 4π events (the errors are taken to be the sqrt of the yields). These numbers are then scaled appropriately to give the expected number of total bkg events in the reconstructed data sample and no error on the scaling factors is assumed.

$$B^{peak}_{tot}(K^0_L\pi\pi\, vs\, K^0_S\pi\pi) = 0.105 \cdot 98 + 0.05 \cdot 419 = 31.24 \pm 1.46 \tag{3.3}$$

and

$$B^{peak}_{tot}(K^0_S\pi\pi\, vs\, 4\pi) = 0.105 \cdot 15 + 0.05 \cdot 90 = 18.45 \pm 0.62 \tag{3.4}$$

Since the branching fraction of $D \to K^0_L\pi\pi$ is unknown, the fraction of $K^0_L\pi\pi$ events in the gen MC sample can't be completely accurate. This can be accounted for by applying a systematic to the number of events obtained from the gen MC (for example assuming that the branching fraction used by CLEO is 20% too small/big).

3.3.2 Relative amount of $K^0_L\pi\pi$ vs $K^0_S\pi\pi$ background events per bin

As for the $K^0_S\pi\pi$ vs $K^0_S\pi\pi$ bkg in $K^0_S\pi\pi$ vs 4π the distribution of $K^0_L\pi\pi$ vs $K^0_S\pi\pi$ events per bin is determined by applying a 'reversed K^0_S veto' on the data. The gen MC sample suggests that after the reversed K^0_S veto sample contains:

- $K^0_L\pi\pi$ vs $K^0_S\pi\pi$: 92%
- flat events: 5%
- $K^0_L\pi\pi$ vs 4π: 1.5%
- $K^0_S\pi\pi$ vs $K^0_S\pi\pi$: 1.5%

The last two are neglected for now (a systematic could be appointed later).

In order to obtain the distribution of $K^0_L\pi\pi$ vs $K^0_S\pi\pi$ events over the bins, the contribution of flat bkg events is estimated as in Section 2.4 and removed from the data. The resulting relative amount of $K^0_L\pi\pi$ vs $K^0_S\pi\pi$ events per bin is shown below.

bin i	a_i^{peak} [%]	$\sigma_a(MC\ stat.)$ [%]	$\sigma_a(data\ stat.)$ [%]
1	31.12	± 0.03	± 2.52
2	11.45	± 0.01	± 1.73
3	7.64	± 0.01	± 1.44
4	3.22	± 0.01	± 0.96
5	10.85	± 0.01	± 1.69
6	5.86	± 0.01	± 1.28
7	12.65	± 0.01	± 1.81
8	16.75	± 0.01	± 2.03

Table 3.2: *Relative amount of $K^0_L\pi\pi$ vs $K^0_S\pi\pi$ events per bin in the data sample with the 'reversed K^0_S veto'. Statistical errors from MC and from data are listed separately.*

3.3.2.1 Selection-bias

Unfortunately 'reversed K^0_S veto' introduced a bias in the distribution of expected $K^0_L\pi\pi$ vs $K^0_S\pi\pi$ events over the bins.
To compensate for this bias the values in Table 3.2 are being weighted with the ratio of reversed K^0_S veto over the K^0_S veto efficiencies determined from the $K^0_L\pi\pi$ vs $K^0_S\pi\pi$ signal MC sample. The weighting factors are listed below.

bin i	*weight*
1	0.94 ± 0.10
2	1.00 ± 0.22
3	1.34 ± 0.38
4	0.70 ± 0.25
5	1.09 ± 0.20
6	1.15 ± 0.26
7	0.77 ± 0.20
8	1.14 ± 0.20

Table 3.3: *Amount by which the numbers in Table 3.2 have to be weighted to compensate for the bias introduced by the Ks-Selection cut.*

The bias introduced by the reversed K^0_S veto has not been removed here due to current lack of $K^0_L\pi\pi$ vs $K^0_S\pi\pi$ signal MC reconstructed as $K^0_L\pi\pi$ vs 4π. We can either apply a systematic on this or generate and reconstruct the needed MC.

3.3.3 Relative amount of $K^0_S\pi\pi$ vs 4π background events per bin

The 'true' distribution of $K^0_S\pi\pi$ vs 4π events in phasespace is taken from the results of the $K^0_S\pi\pi$ vs 4π analysis, namely the values of Table 2.8.

This distribution is weighted to account for the bin-dependent selection and reconstruction efficiency.

The efficiency for reconstructing and selecting $K^0_S\pi\pi$ vs 4π events as $K^0_L\pi\pi$ vs 4π events is taken to be the same as that for genuine $K^0_L\pi\pi$ vs 4π events - under the assumption the K^0_S is 'lost' which should result in the same kinematics of the two decays. (If this explanation seems dodgy we can try and get some $K^0_S\pi\pi$ vs 4π signal MC to be reconstructed as $K^0_L\pi\pi$ vs 4π.)

bin i	a_i^{peak} [%]	$\sigma_a(MC\ stat.)$ [%]	$\sigma_a(data\ stat.)$ [%]
1	14.86	± 0.14	± 3.52
2	9.29	± 0.22	± 2.52
3	6.91	± 0.23	± 1.92
4	4.79	± 0.24	± 1.66
5	24.50	± 0.28	± 4.36
6	10.34	± 0.57	± 2.61
7	12.80	± 0.31	± 2.97
8	16.51	± 0.39	± 3.41

Table 3.4: *Relative amount of $K^0_S\pi\pi$ vs 4π events per bin in the data sample with the 'reversed K^0_S veto'. Statistical errors from MC and from data are listed separately.*

3.3.4 Resulting number of peaking background events in selected data sample

Applying these scaling values to the factors a_i yields the total amount of peaking bkg contamination in the data sample listed below.

bin i	$B_i^{peak}(K^0_L\pi\pi\ vs\ K^0_S\pi\pi)$	$B_i^{peak}(K^0_S\pi\pi\ vs\ 4\pi)$
1	9.12 ± 2.15 ± 0.74	0.90 ± 0.37 ± 0.21
2	3.59 ± 1.09 ± 0.54	0.56 ± 0.23 ± 0.15
3	3.20 ± 1.12 ± 0.61	0.42 ± 0.17 ± 0.12
4	0.701 ± 0.29 ± 0.21	0.29 ± 0.12 ± 0.10
5	3.69 ± 1.03 ± 0.58	1.49 ± 0.61 ± 0.26
6	2.10 ± 0.65 ± 0.46	0.63 ± 0.26 ± 0.16
7	3.02 ± 1.02 ± 0.43	0.78 ± 0.32 ± 0.18
8	5.96 ± 1.61 ± 0.72	1.00 ± 0.41 ± 0.21

Table 3.5: *Number of peaking background events per bin in the data sample. The errors are statistical only, first error from MC and the second one from data.*

3.4 Determination of number of flat and continuum background events

The total number of flat bkg events and continuum bkg events is determined using a form of the 'Powell method' (see Chris's thesis). In this derivation the raw event yield D_i in sideband i is expressed as:

$$D_i = T_{Si} + T_{Pi} + T_{Fi} + T_{Ci} \tag{3.5}$$

where T_{Si} denotes the raw signal yield in sideband i, T_Pi the raw yields of peaking bkg events, T_Fi the raw yields of flat bkg events and T_{Ci} the raw yields of continuum events. That means instead of dividing the flat bkg into 'peaking in low sideband' and 'peaking in high sideband' the bkg is divided into continuum and flat bkg. The assumption that the ratios of signal, continuum bkg and flat bkg per bin in data are the same as in MC should also hold here.

The errors on the number of flat bkg events and continuum bkg events are determined by varying the input values according to a Poisson distribution 10 000 times. This results in 28.42 ± 10.80 ± 6.80 flat bkg events in the data sample and 37.15 ± 10.85 ± 9.45 continuum events, where the first error is the statistical error from MC and the second one from data.

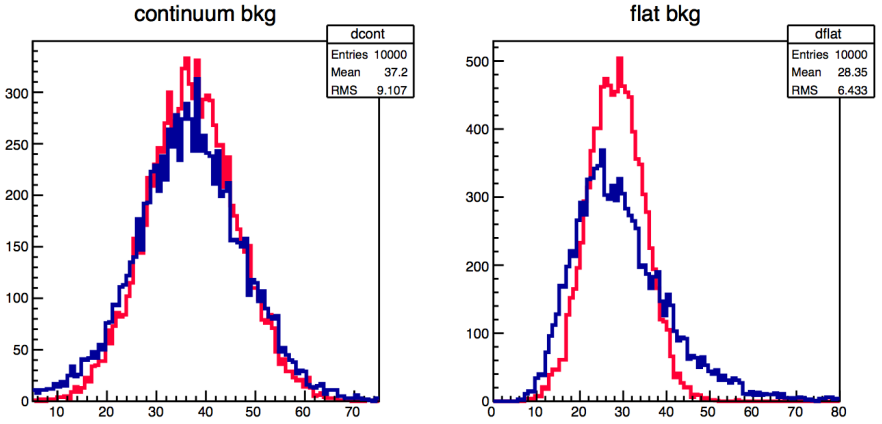

Figure 3.2: *Distribution of total number of continuum and flat bkg events in the data sample determined with the Powell method. Red distribution: varying the MC input, blue distribution: varying the data input.*

The continuum bkg is assumed to be flat in phasespace, so the 37 events are distributed across the bins according to Table 2.2. This results in the following number of continuum events per bin:

bin i	B_i^{cont}	$\sigma_{B_i^{cont}}(MC\ stat)$	$\sigma_{B_i^{cont}}(data\ stat)$
1	12.28	± 3.59	± 3.12
2	4.24	± 1.24	± 1.08
3	2.37	± 0.69	± 0.60
4	2.20	± 0.64	± 0.56
5	4.95	± 1.44	± 1.26
6	3.00	± 0.88	± 0.76
7	3.13	± 0.91	± 0.80
8	4.98	± 1.46	± 1.27

Table 3.6: *Number of continuum bkg events per bin in the data sample.*

The number of flat bkg events in bin i are then:

bins	B_i^{flat}	$\sigma_{B_i^{flat}}(MC\ stat)$	$\sigma_{B_i^{flat}}(data\ stat)$
1	9.39	± 3.57	± 2.25
2	3.24	± 1.23	± 0.78
3	1.82	± 0.69	± 0.43
4	1.68	± 0.64	± 0.40
5	3.79	± 1.44	± 0.91
6	2.30	± 0.87	± 0.55
7	2.39	± 0.91	± 0.57
8	3.81	± 1.45	± 0.91

Table 3.7: *Number of flat bkg events per bin in the data sample.*

3.5 Determination of the signal selection-efficiency

The signal selection efficiency in each bin is determing using a sample of 50 000 $K^0_L\pi\pi$ vs 4π signal MC events.
The results are listed below.

bin	ϵ [%]
1	23.87 ± 0.33
2	23.20 ± 0.56
3	20.85 ± 0.72
4	23.19 ± 0.78
5	21.90 ± 0.51
6	24.24 ± 0.67
7	23.00 ± 0.65
8	22.10 ± 0.51

Table 3.8: *Signal efficiency per bin.*

3.6 Resulting MM_i

Since M_i and M_{-i} are the same, the numbers are directly evaluated for the sum of M_i and M_{-i} and listed on the table below.

bin	MM_i
1	512.33 ± 24.16 ± 54.52
2	204.17 ± 10.19 ± 33.69
3	202.33 ± 10.02 ± 34.23
4	78.20 ± 4.89 ± 20.92
5	164.73 ± 11.46 ± 33.18
6	82.38 ± 6.30 ± 22.26
7	268.10 ± 10.49 ± 36.93
8	277.09 ± 13.55 ± 40.47

Table 3.9: *M_i + M_{-i} The first error is from the MC statistics and the second one from the data statistics.*

3.7 Summary

bin	raw yields	$B_i^{peak}(K^0_L\pi\pi\, vs\, K^0_S\pi\pi)$	$B_i^{peak}(K^0_S\pi\pi\, vs\, 4\pi)$	B_i^{cont}	B_i^{flat}	signal
1	154	9.12	0.90	12.28	9.39	122.30
2	59	3.59	0.56	4.24	3.24	47.37
3	50	3.20	0.42	2.37	1.82	42.19
4	23	0.70	0.29	2.20	1.68	18.13
5	50	3.69	1.49	4.95	3.79	36.08
6	28	2.10	0.63	3.00	2.30	19.97
7	71	3.02	0.78	3.13	2.39	61.67
8	77	5.96	1.00	4.98	3.81	61.24

Table 3.10: *Summary of contributions to the raw yields per bin.*

4. Fit for F_+

4.1 Fractional flavour-tagged $K^0_S\pi\pi$ yields T_i

The given values for K'_i obtained from Table 1 of `arXiv:1210.939` contain effects from charm-mixing that cancel in our case. The factors T_i without mixing are archived by numerically solving the system of equations:

$$K'_i = T_i + \sqrt{T_i T_{-i}}(yc_i + xs_i) \tag{4.1}$$

where x and y charm-mixing parameters. The fit also takes into account that the sum over the T_i should be one by fixing $T_1 = 1 - \sum_{i\neq 1} T_i$. The values for x and y are take from the latest HFAG results ($x = (0.63 \pm 0.19)\%$, $y = (0.75 \pm 0.12)\%$) and the values for c_i and s_i are taken from `arXiv:1010.2817`. In the fit all input variables are Gaussian constraint and the correlation between c_i and s_i are taken into account. The resulting T_i are listed below.

bin	T_i	bin	T_i
1	0.1695 ± 0.0053	-1	0.0781 ± 0.0014
2	0.0873 ± 0.0012	-2	0.0186 ± 0.0002
3	0.0723 ± 0.0020	-3	0.0201 ± 0.0003
4	0.0258 ± 0.0011	-4	0.0161 ± 0.0015
5	0.0889 ± 0.0024	-5	0.0523 ± 0.0013
6	0.0589 ± 0.0011	-6	0.0147 ± 0.0003
7	0.1252 ± 0.0018	-7	0.0132 ± 0.0004
8	0.1320 ± 0.0021	-8	0.0270 ± 0.0010

Table 4.1: *Fraction flavour-tagged $K^0_S\pi\pi$ yields without mixing-effects.*

4.2 Fractional flavour-tagged $K^0_L\pi\pi$ yields T'_i

The fractional flavour-tagged $K^0_L\pi\pi$ yields are taken from Sean Brisbane's thesis (Section 3., Table 3.14). They are listed below:

bin	T'_i	bin	T'_i
1	0.163 ± 0.004	-1	0.090 ± 0.017
2	0.069 ± 0.003	-2	0.024 ± 0.005
3	0.061 ± 0.003	-3	0.031 ± 0.006
4	0.026 ± 0.002	-4	0.019 ± 0.004
5	0.082 ± 0.003	-5	0.057 ± 0.014
6	0.058 ± 0.002	-6	0.017 ± 0.004
7	0.122 ± 0.003	-7	0.021 ± 0.003
8	0.124 ± 0.003	-8	0.035 ± 0.008

Table 4.2: *Fraction flavour-tagged $K^0_L\pi\pi$ yields.*

4.3 F_+ from $K^0_S\pi\pi$

The fit to the $K^0_S\pi\pi$ data only yields $F_+ = 0.841 \pm 0.070$ and a normalisation term h for $K^0_S\pi\pi$ of $h = 681.48 \pm 51.69$. The χ^2_{ndof} for this fit is 0.56.

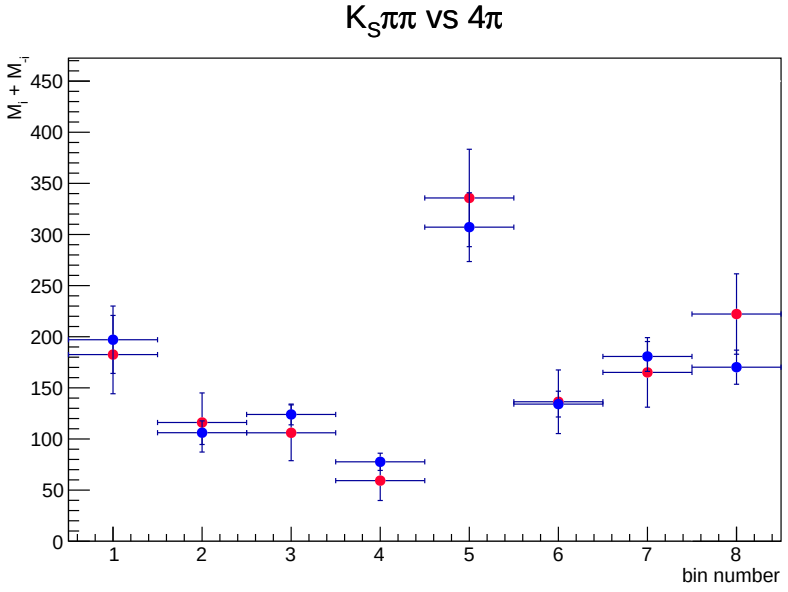

Figure 4.1: *Distribution of $MM^{K^0_S\pi\pi}$ over the bins. Red: data, blue: fit values.*

4.4 F_+ from $K^0_L\pi\pi$

The fit to the $K^0_L\pi\pi$ data only yields $F_+ = 0.677 \pm 0.063$ and a normalisation term h for $K^0_L\pi\pi$ of $h = 866.53 \pm 57.94$. The χ^2_{ndof} for this fit is 0.48.

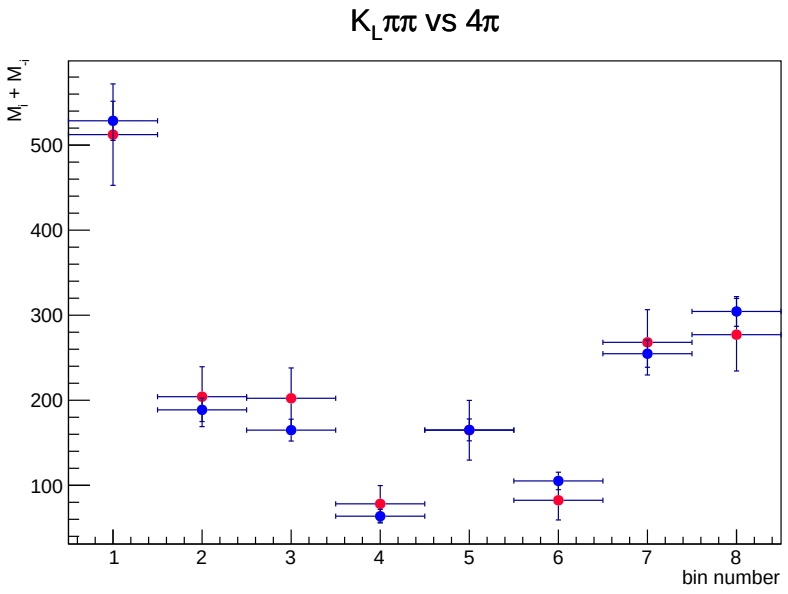

Figure 4.2: *Distribution of $MM^{K^0_L\pi\pi}$ over the bins. Red: data, blue: fit values.*

4.5 F_+ from simultaneous fit

The fit to both the $K^0_S\pi\pi$ and $K^0_L\pi\pi$ data yields $F_+ = 0.744 \pm 0.048$ and normalisation terms $h_{K^0_S\pi\pi} = 662.67 \pm 50.66$ and $h_{K^0_L\pi\pi} = 858.24 \pm 58.94$. The χ^2_{ndof} for this fit is 0.66.

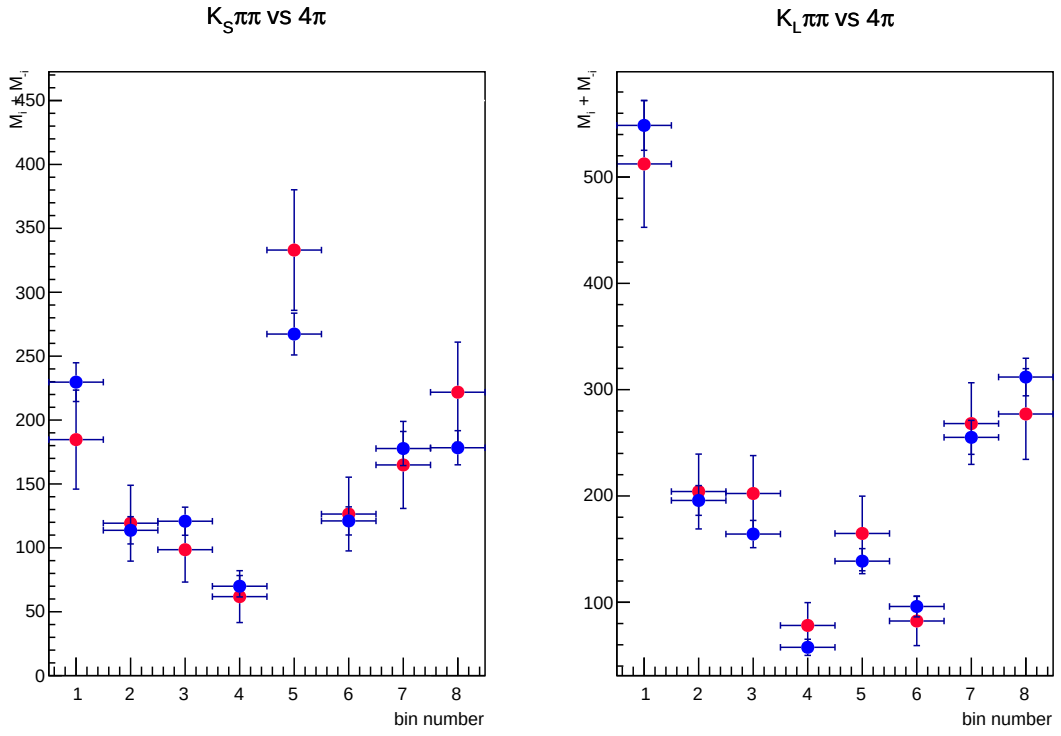

Figure 4.3: *Distribution of $MM^{K^0_S\pi\pi}$ and $MM^{K^0_L\pi\pi}$ over the bins. Red: data, blue: fit values.*

What might be noteworthy is that some T_i' values for the $K_L^0\pi\pi$ get stretched quite a bit by the fit, especially T'_{-4}. The table below shows how much each of the input variables gets changed by the fit:

input variable	shift [%]	shift/σ_{fit}	$\sigma_{fit}/\sigma_{input}$
c_1	0.36	0.12	0.35
c_2	0.38	0.062	0.34
c_3	23	0.14	0.24
c_4	-1.2	0.13	0.35
c_5	-0.23	0.093	0.36
c_6	-0.33	0.054	0.3
c_7	7.9	0.15	0.33
c_8	0.32	0.04	0.33
T_1	-0.52	-0.17	0.99
T_2	0.012	0.0087	1
T_3	-0.24	-0.09	1
T_4	-0.14	-0.035	1
T_5	0.34	0.13	1
T_6	0.02	0.011	1
T_7	-0.037	-0.026	1
T_8	0.12	0.072	1
T_{-1}	-0.05	-0.029	1
T_{-2}	0.00084	0.00077	1
T_{-3}	-0.022	-0.014	1
T_{-4}	-0.52	-0.055	0.99
T_{-5}	0.19	0.079	1
T_{-6}	0.0085	0.0041	1
T_{-7}	-0.015	-0.005	1
T_{-8}	0.073	0.02	1
T'_1	-0.21	-0.086	1
T'_2	0.17	0.04	0.99
T'_3	0.77	0.16	0.99
T'_4	0.9	0.12	0.99
T'_5	0.25	0.068	1
T'_6	-0.25	-0.074	0.99
T'_7	0.11	0.047	0.99
T'_8	-0.26	-0.11	0.99
T'_{-1}	-8.1	-0.48	0.9
T'_{-2}	1.7	0.087	0.95
T'_{-3}	6.1	0.33	0.96
T'_{-4}	4.4	0.21	0.98
T'_{-5}	6.1	0.25	0.97
T'_{-6}	-1.8	-0.079	0.99
T'_{-7}	0.73	0.051	0.99
T'_{-8}	-8.4	-0.39	0.94

Table 4.3: *Amount by which the Gaussian constraint input variables are shifted in the fit.*